iRIS 중이온가속기연구소 Institute for Rare Isotope Science

Ongoing Development of Single-Spoke Resonator Type 1 Superconducting Cavities at RAON

TTC2025 Meeting
IRIS/IBS, Daejeon, Korea
April 9, 2025 (11:00-11:30)

Heetae Kim
on behalf of the High-Energy Linac Development Team
Institute for Rare Isotope Science (IRIS)
Institute for Basic Science (IBS), Korea

Contents

Vertical Test Facility

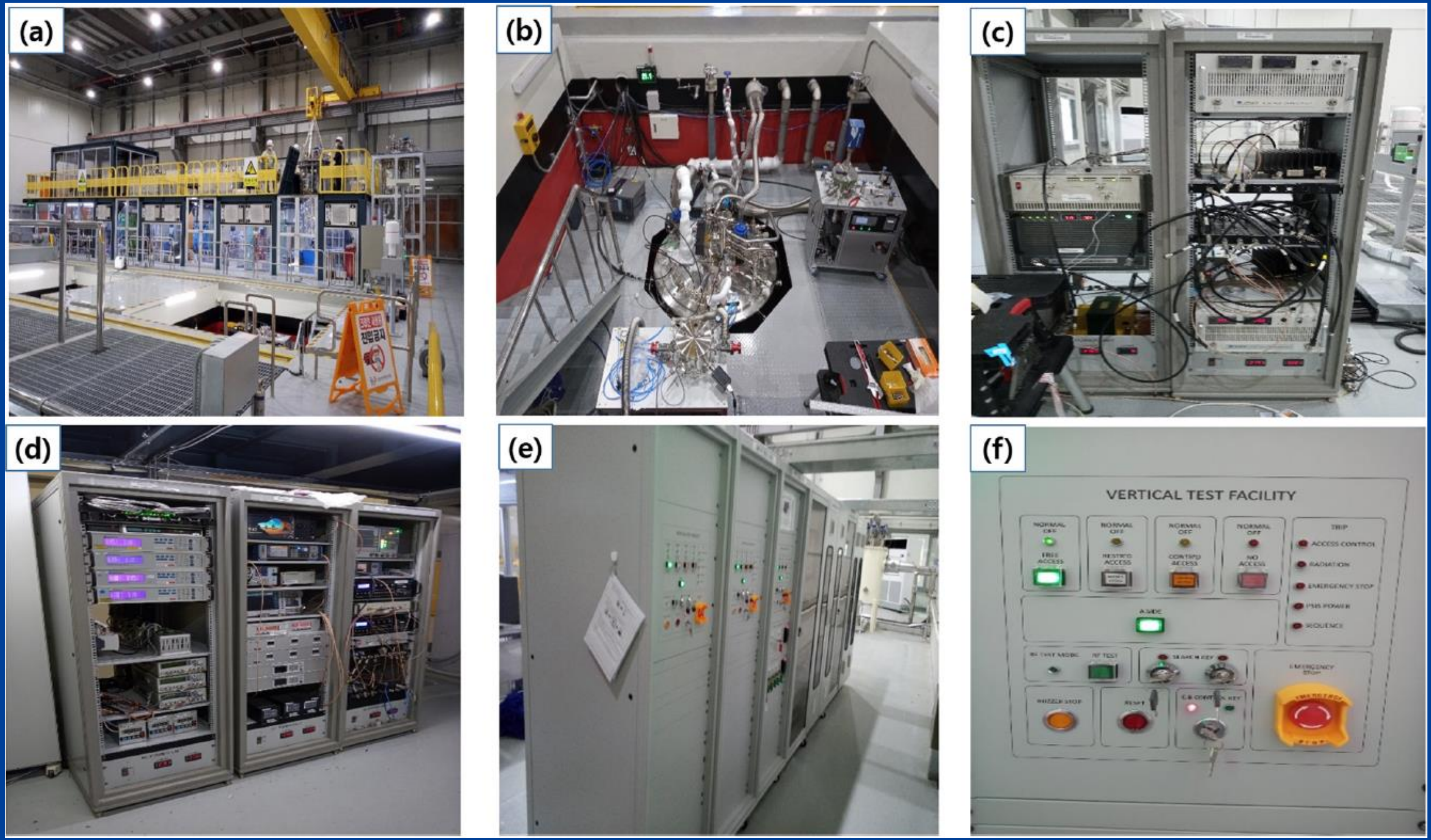

Figure: Photographs of the vertical test facility. (a) Overview of the vertical test site; (b) Vertical test pit and cryostat; (c) Solid-state power amplifier (SSPA); (d) Control racks; (e) Personal safety interlock system (PSIS); (f) Control panel for the PSIS.

Sungmin Jeon, Heetae Kim*, Yoochul Jung, Juwan Kim, Junwoo Lee, Moosang Kim, Hyunik Kim, Sangbeen Lee, Minki Lee, Field emission and x-ray effect on RAON HWR superconducting cavity performance, Current Applied Physics 38, 67-75 (2022).

Vertical Test Facility

Figure: Top view showing the hanging booth, the top flange inserted into the pit, control racks, and the control room.

Vertical Test Facility

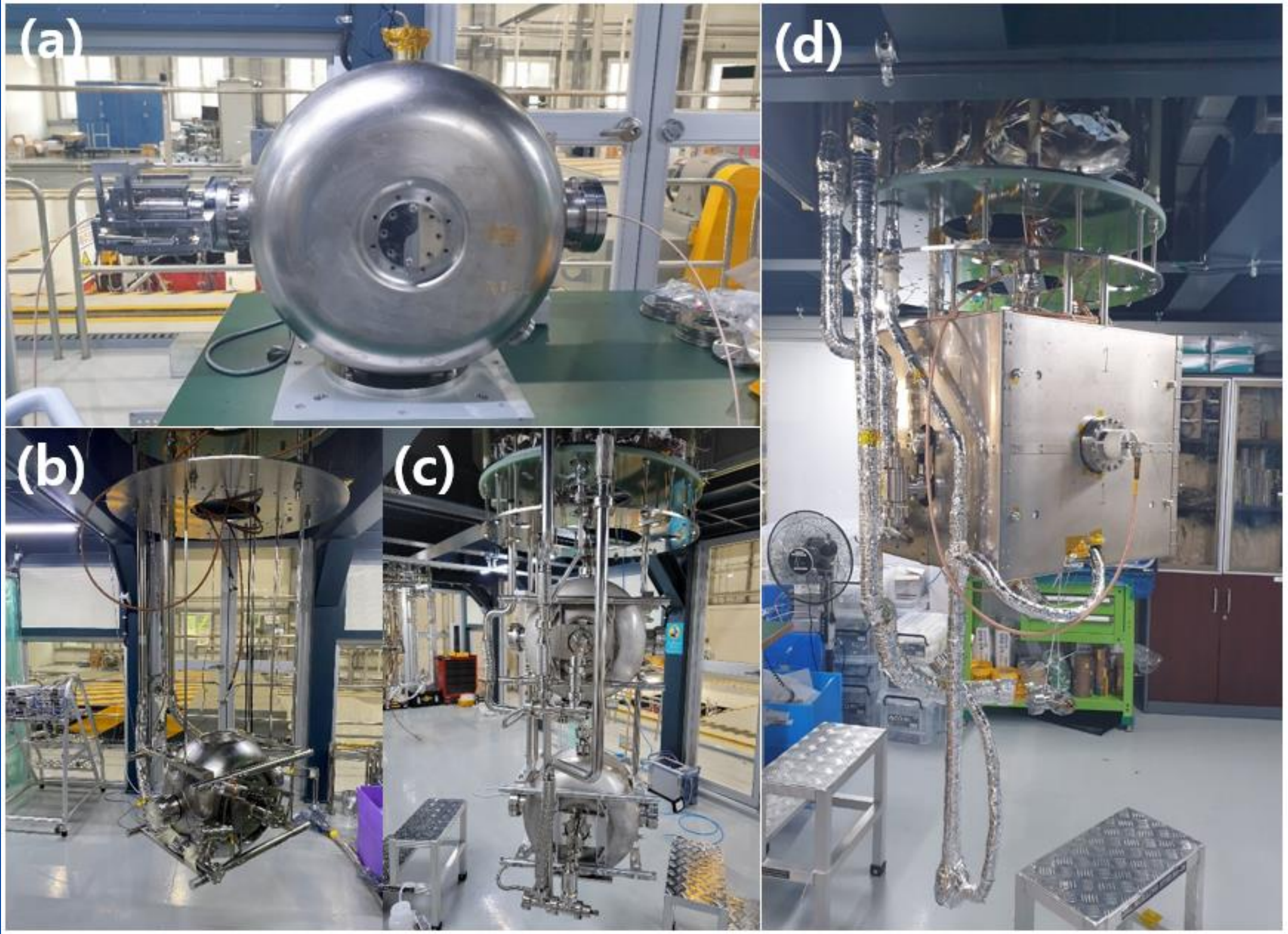

Figure: Images of single-spoke resonators (SSRs). (a) SSR cavity with a jacket; (b) SSR cavity without a jacket; (c) Multiple SSR cavities with jackets; (d) SSR cavity with magnetic shielding.

Heetae Kim, Juwan Kim, Sungmin Jeon, Junwoo Lee, Moosang Kim, Heecheol Park, Yoochul Jung, Performance test for single-spoke resonator superconducting cavities in RAON, IPAC 2024, MOPC34, 136-139 (2024).

Images of a Superconducting Cavity SSR1

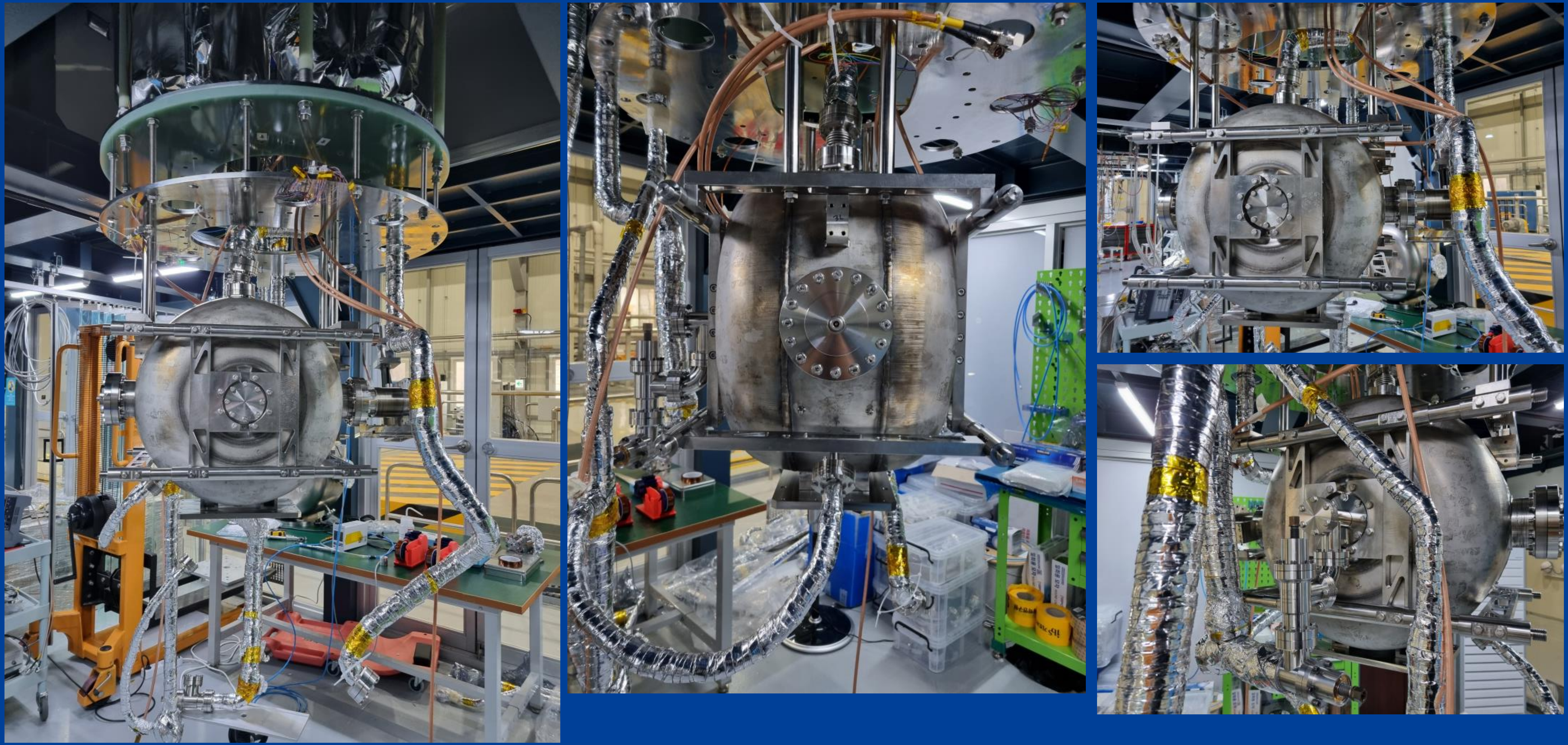

Figure: Image of a single-spoke resonator (SSR1) with a jacket.

Cryogenic System and Cryostat

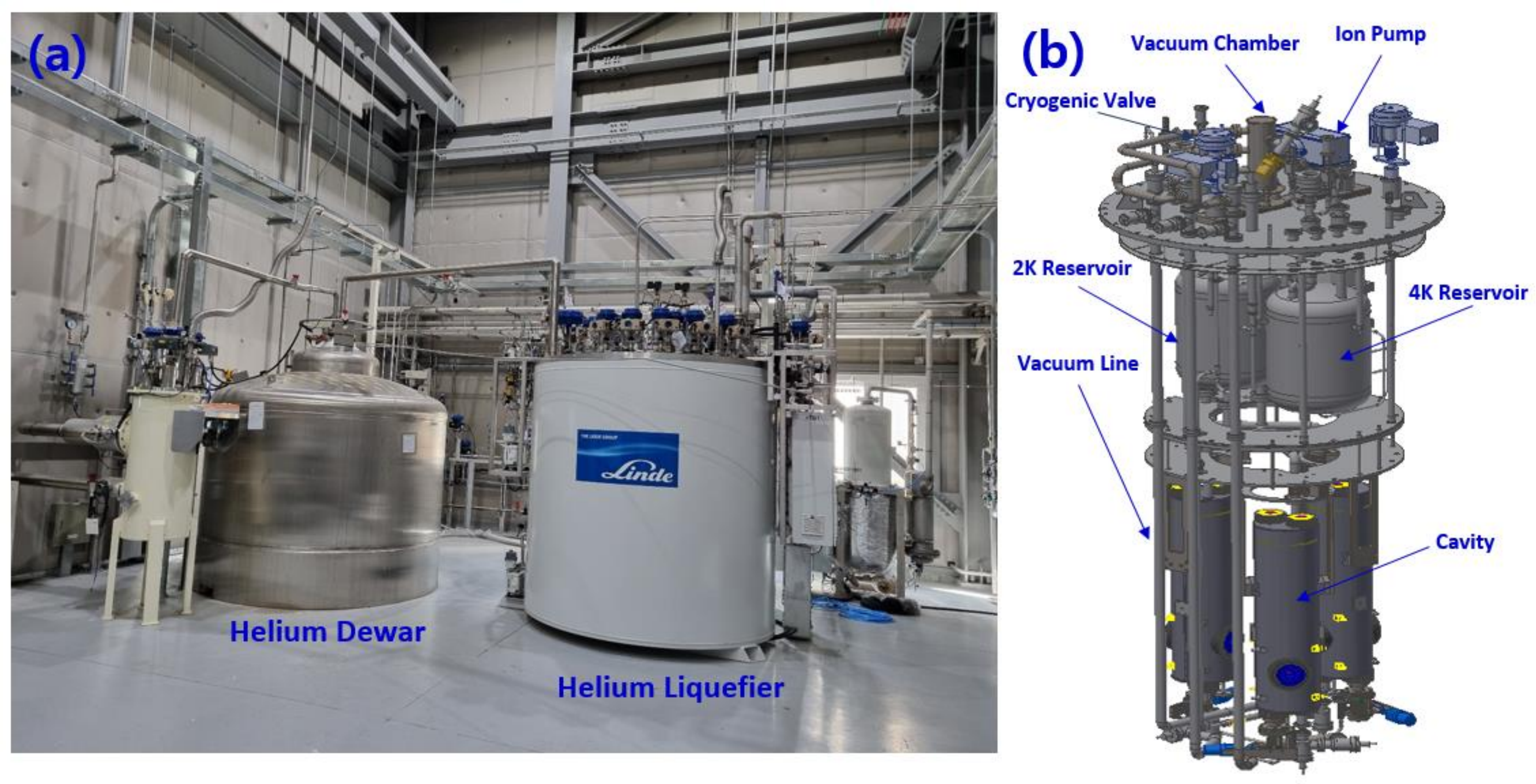

Figure: Cryogenic system and cryostat. (a) Helium liquefier and helium dewar; (b) Cryostat.

The cryogenic system includes a helium liquefier (280 L/h capacity), a liquid helium dewar (3,000 L capacity), warm pumps for 2 K pumping (1.5 g/s per pump), recovery compressors, gas bags, and a liquid nitrogen tank.

Heetae Kim, Juwan Kim, Sungmin Jeon, Junwoo Lee, Moosang Kim, Heecheol Park, Yoochul Jung, Performance test for single-spoke resonator superconducting cavities in RAON, IPAC 2024, MOPC34, 136-139 (2024).

Parameters for a Single-Spoke Resonator type 1 (SSR1) Cavities

Parameter	SSR1
β_{OPT}	0.32
f (MHz)	325
$L_{eff}(= \beta_0\lambda)(mm)$	276.9
R/Q (Ω)	233
E_{peak}/E_{acc}	4.1
B_{peak}/E_{acc} **[mT/(MV/m)]**	6.9
E_{acc} **(MV/m)**	8.5
V_{acc} **(MV)**	2.35
Stored energy (J)	11.6
QR_s	92.2
kappa	55.13

Performance Test Procedures

Performance Test Procedures

1. Welded jacketed cavity preparation
2. Light Buffered Chemical Polishing (BCP)
3. High-Pressure Rinsing (HPR)
4. Low-Temperature Baking (120 °C for 48 hours)
5. Cool-down to 4.2 K
   - Rapid cooling between 150 K and 50 K
6. RF Conditioning
7. Performance Test at 4.2 K
   - Q curve and Lorentz Force Detuning (LFD)
8. Pressure Sensitivity Measurement
9. Performance Test at 2 K
   - Q curve and Lorentz Force Detuning (LFD)

Experimental Setup for the Vertical Test

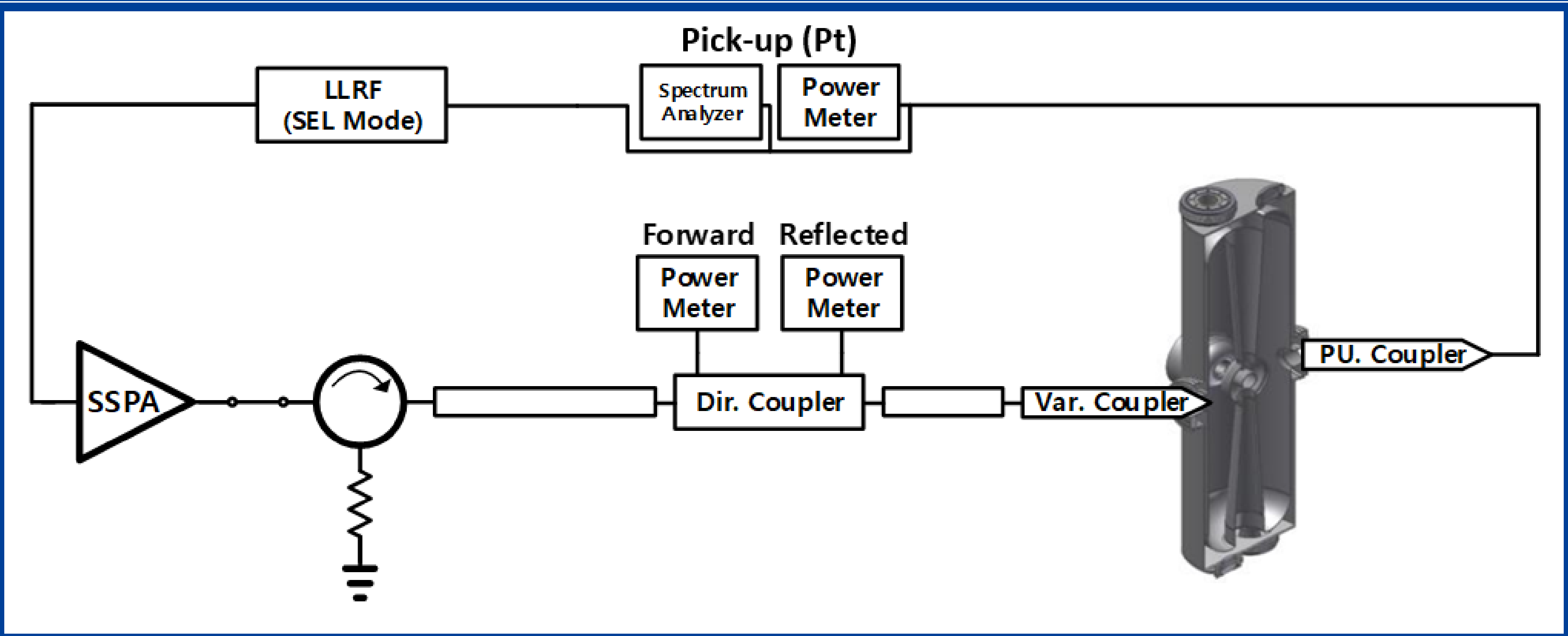

Figure: Experimental setup for the vertical test. The solid-state power amplifiers (SSPAs) have power ratings of 200 W and 500 W. RF power is delivered to the superconducting cavity via a variable coupler, and transmitted power is detected through a pickup coupler. Forward and reflected powers are measured using power meters, while the pickup signal is monitored with both a power meter and a spectrum analyzer.

Heetae Kim, Sungmin Jeon, Juwan Kim, Junwoo Lee, Moosang Kim, Jongdae Joo, Myung Ook Hyun, Hoe Chun Jung, Hyojae Jang, Youngkwon Kim, Gunn-Tae Park, Mijoung Joung, Yoochul Jung, Superconducting cavities for SCL3, J. Korean Phys. Soc. (2024). DOI: 10.1007/s40042-024-01267-5

P&ID for the Cryostat

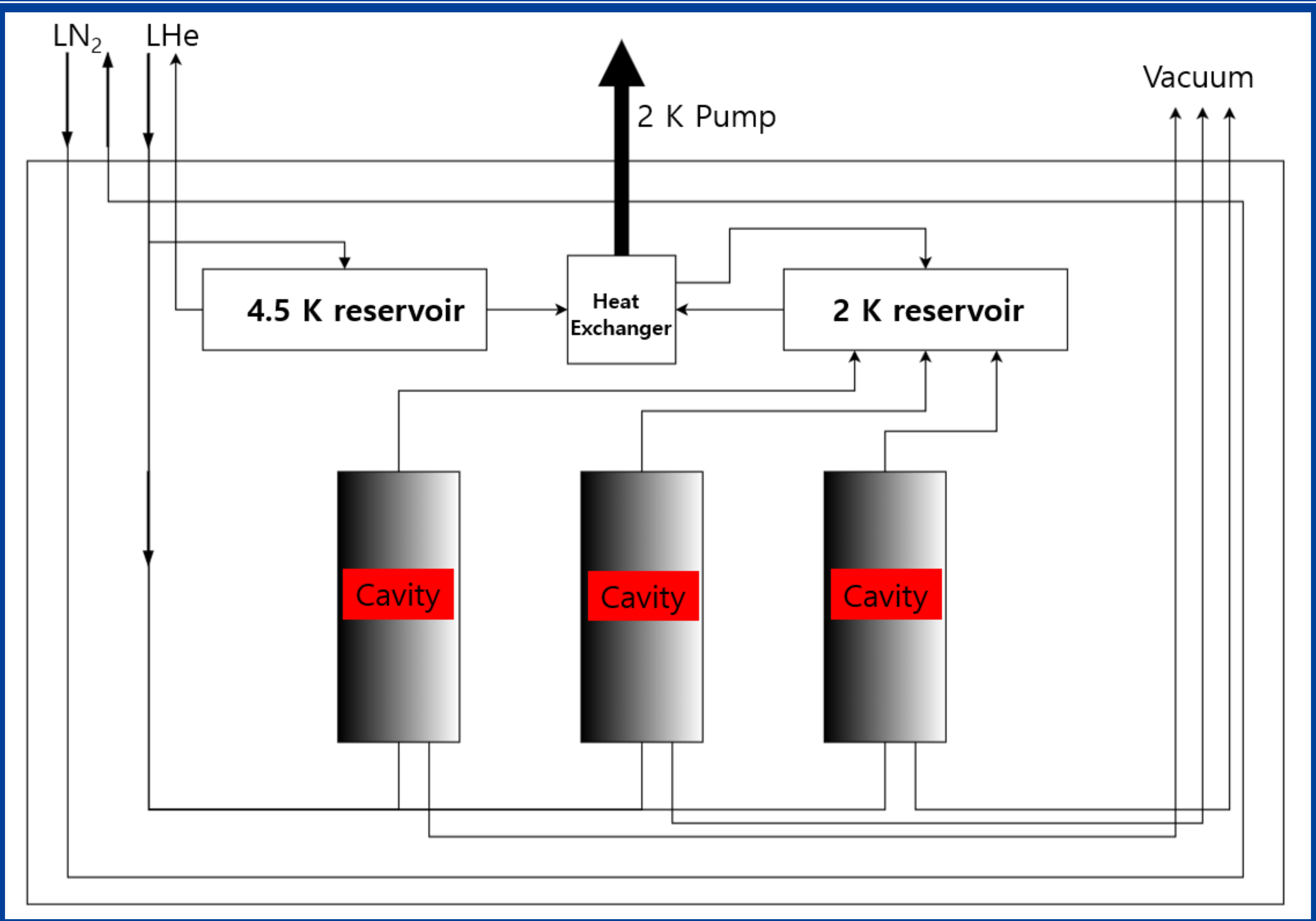

Figure: P&ID diagram of the cryostat during the vertical test.A fast cool-down is conducted in the temperature range of 150 K to 50 K.

Heetae Kim, Sungmin Jeon, Juwan Kim, Junwoo Lee, Moosang Kim, Jongdae Joo, Myung Ook Hyun, Hoe Chun Jung, Hyojae Jang, Youngkwon Kim, Gunn-Tae Park, Mijoung Joung, Yoochul Jung, Superconducting cavities for SCL3, J. Korean Phys. Soc. (2024). DOI: 10.1007/s40042-024-01267-5

Control Panels

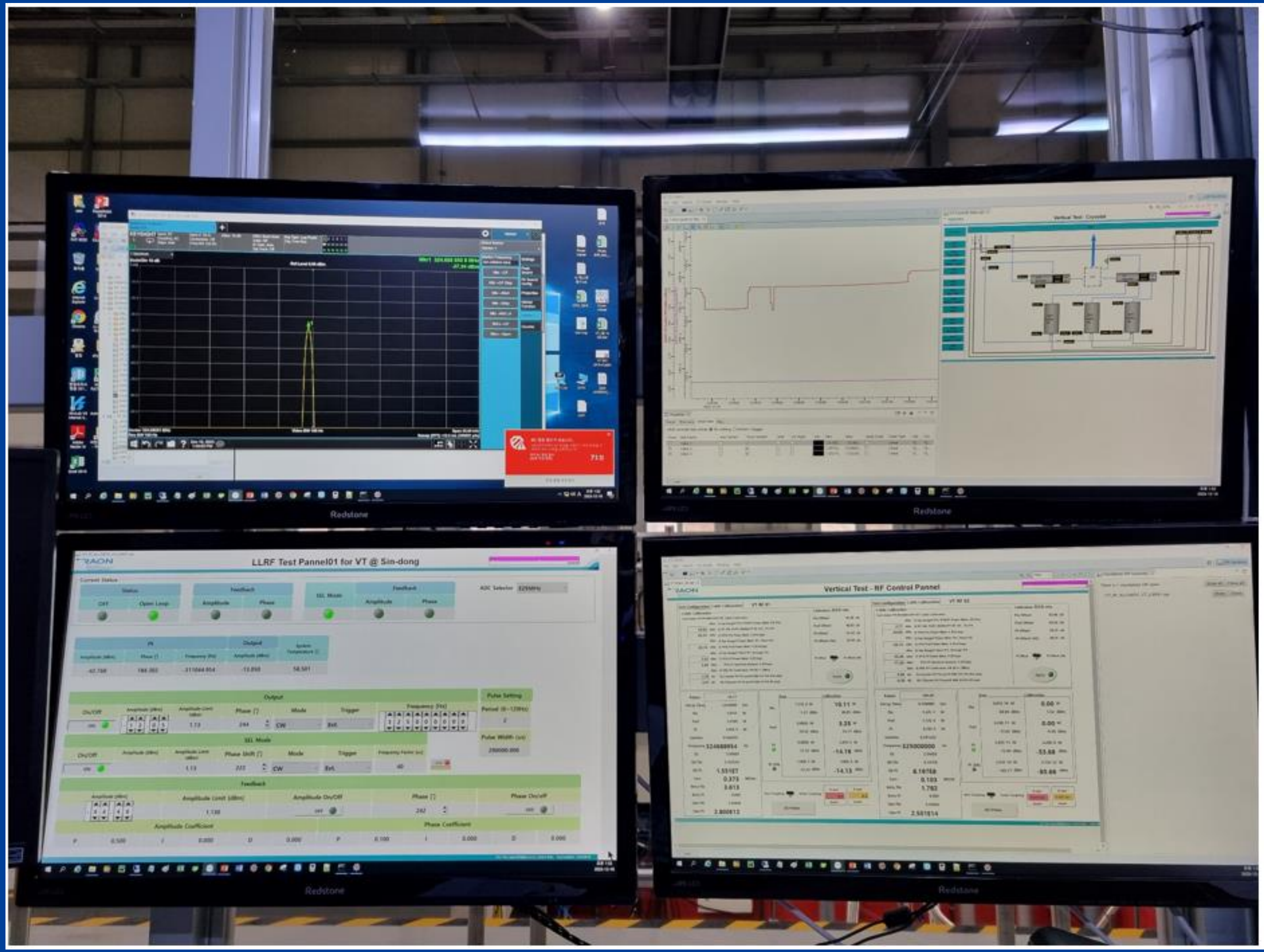

Figure: Control panels used for the vertical test.
The image shows the spectrum analyzer, LLRF test panel, RF control panel, and cryostat monitor.

Heetae Kim, Juwan Kim, Sungmin Jeon, Junwoo Lee, Moosang Kim, Heecheol Park, Yoochul Jung, Performance test for single-spoke resonator superconducting cavities in RAON, IPAC 2024, MOPC34, 136-139 (2024).

RF Conditioning

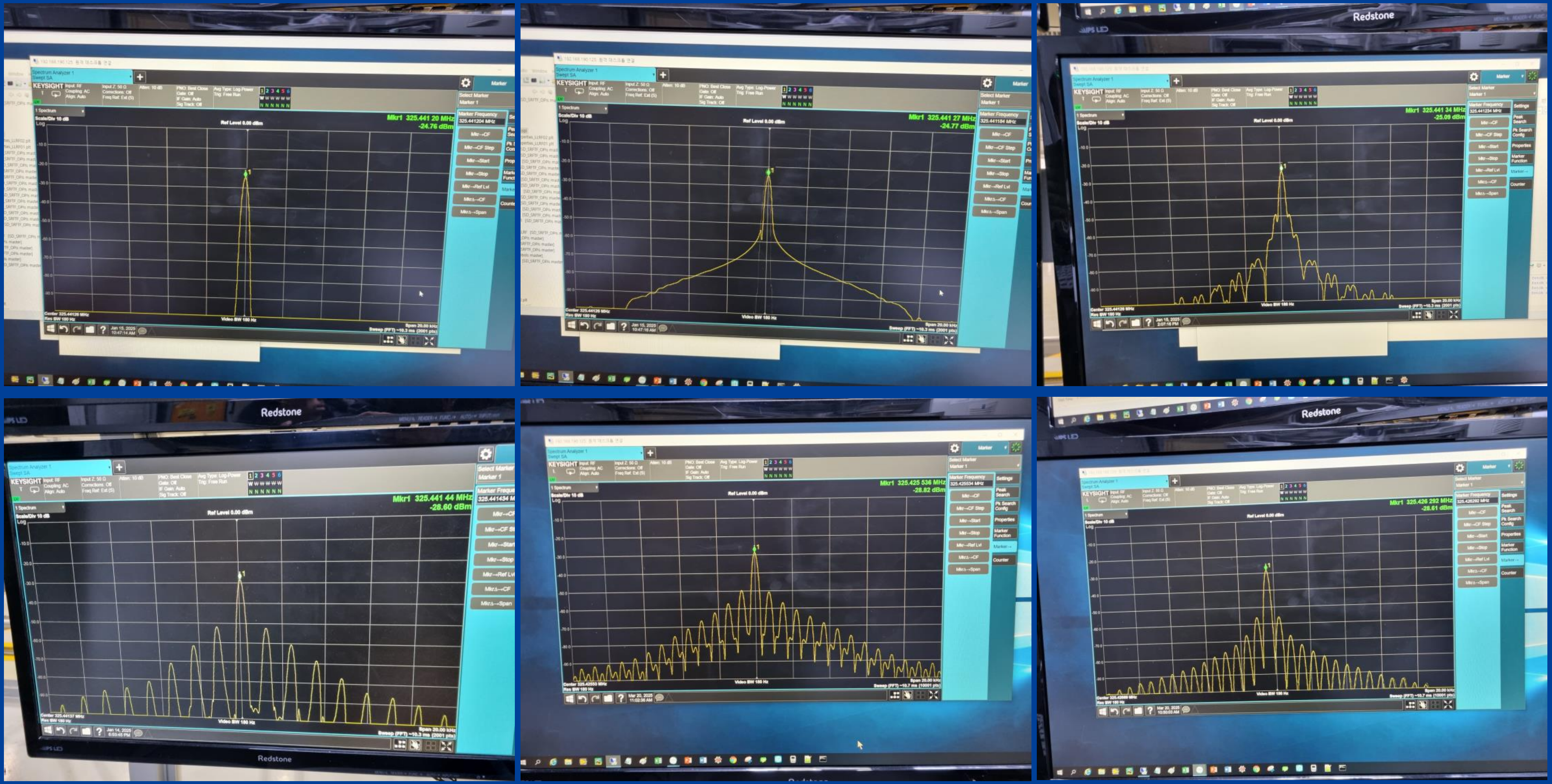

Figure: Spectrum analyzer displays showing various stages of RF conditioning.

Performance Test

Performance test parameters:

- Quality Factor (Q)
- Lorentz Force Detuning (LFD)
- Pressure Sensitivity (df/dp)

Performance tests evaluate the quality factor (Q), Lorentz force detuning (LFD), and pressure sensitivity (df/dp) of the superconducting cavities at their operating temperature.

Quality Factor Invariance Under Relativistic Motion

iRiS 중이온가속기연구소 Institute for Rare Isotope Science

The intensity of the radio frequency in a superconducting cavity decays as follows:

$$I = I_o e^{-\frac{2\pi f t}{Q}}$$

where I_o is the initial intensity, f is the resonance frequency of the cavity, Q is the quality factor, and t is the time.

The quality factor Q can also be expressed as:

$$Q = \frac{2\pi f \tau_{3.01\mathrm{dB}}}{\ln 2}$$

where $\tau_{3.01\mathrm{dB}}$ is the decay time at which the intensity decreases by 3.01 dB (i.e. to half of its initial value) and f is again the resonance frequency.

Quality Factor and Relativistic Invariance

The Q factor is defined as

$$Q(0) = \frac{E}{\Delta E}$$

where E is the energy and ΔE is the width of the energy.

For constant velocity v:

$$Q(v) = \frac{E\sqrt{1-\left(\frac{v}{c}\right)^2}}{\Delta E\sqrt{1-\left(\frac{v}{c}\right)^2}} = \frac{E}{\Delta E}$$

Thus, the Q factor remains unchanged under constant velocity.

For constant acceleration a:

$$Q(a) = \frac{E\sqrt{1-(2ax/c^2)}}{\Delta E\sqrt{1-(2ax/c^2)}} = \frac{E}{\Delta E}$$

where a is the acceleration and x is the distance.
Therefore, the Q factor is conserved in a uniformly accelerated frame.

The Q factor exhibits relativistic invariance.

Heetae Kim, Conservation of quality factor for superconducting cavities and mammals under relativistic motion, J. Korean Phys. Soc. 84, 224-230 (2024).

Quality Factor for Passed SSR1 Cavities

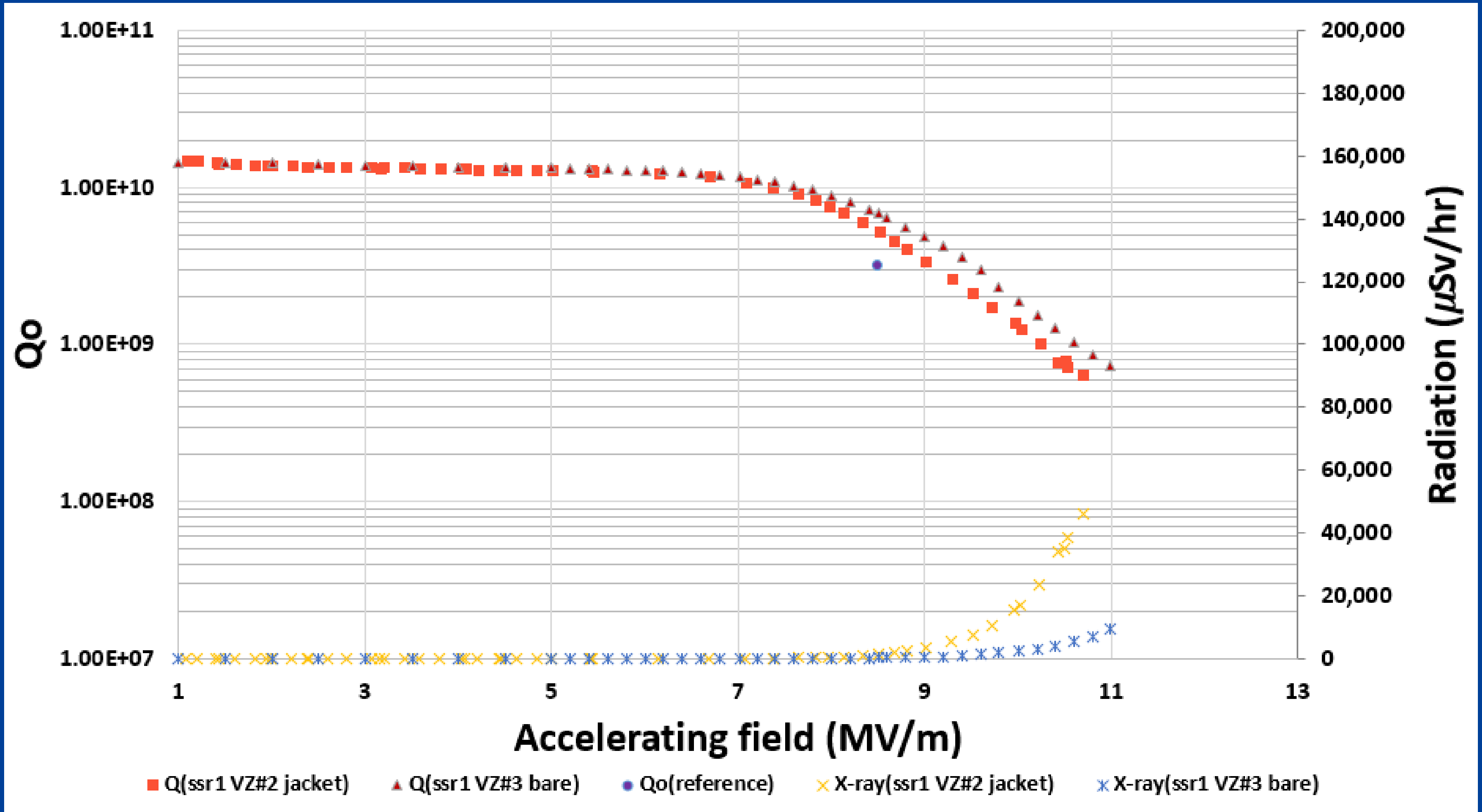

Reference Q= 3.2×10^{9} at 8.5MV/m

Figure: Quality factor as a function of accelerating field.

Two SSR1 cavities successfully passed the vertical qualification test.

Quality Factor and LFD for Ongoing Test

iRiS 중이온가속기연구소 Institute for Rare Isotope Science

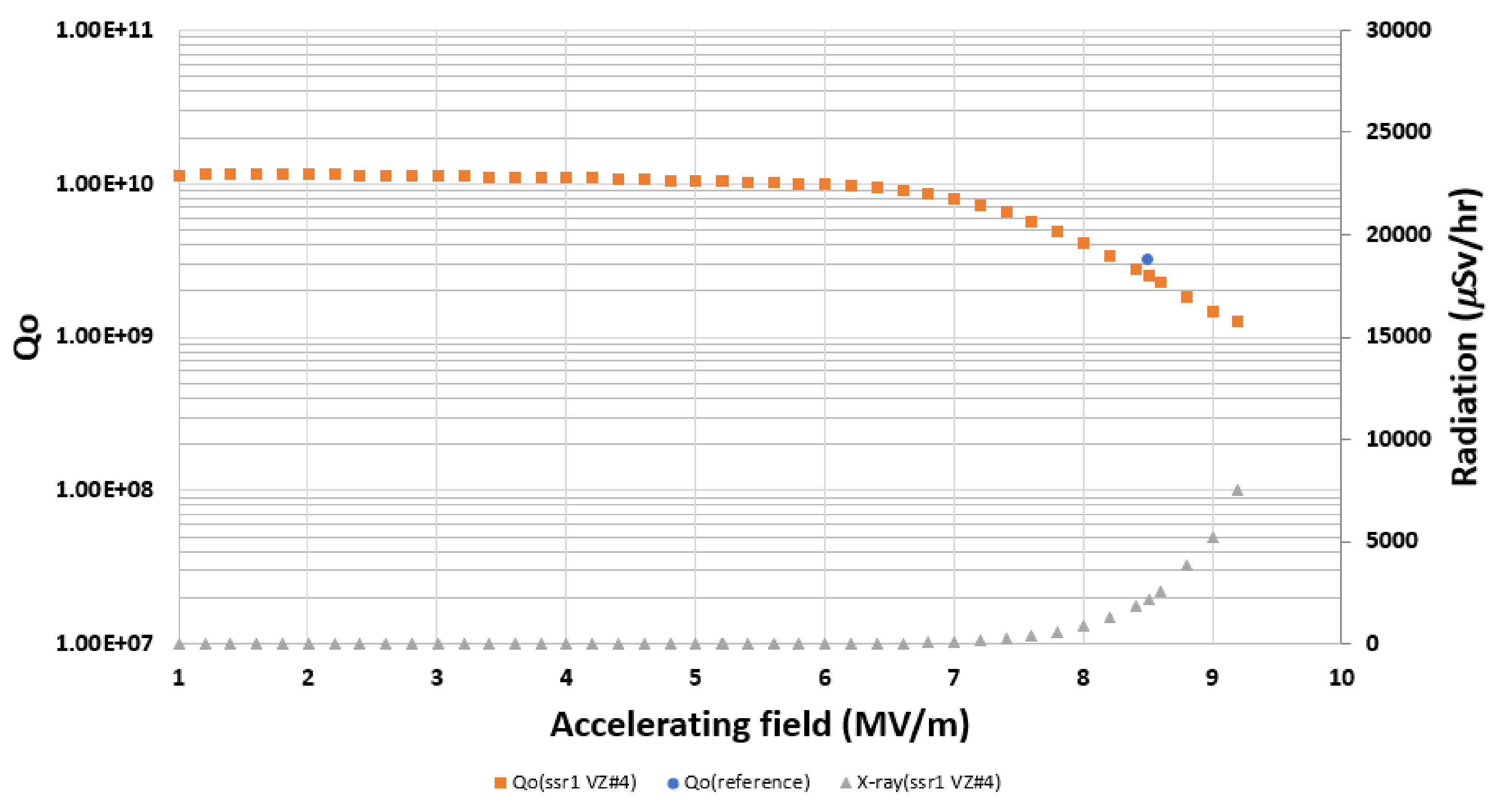

Figure: Quality factor as a function of accelerating field.

The measured Lorentz force detuning (LFD) is -9.7 Hz/$(MV/m)^2$.

Pressure Sensitivity for Ongoing Test

iRIS 중이온가속기연구소 Institute for Rare Isotope Science

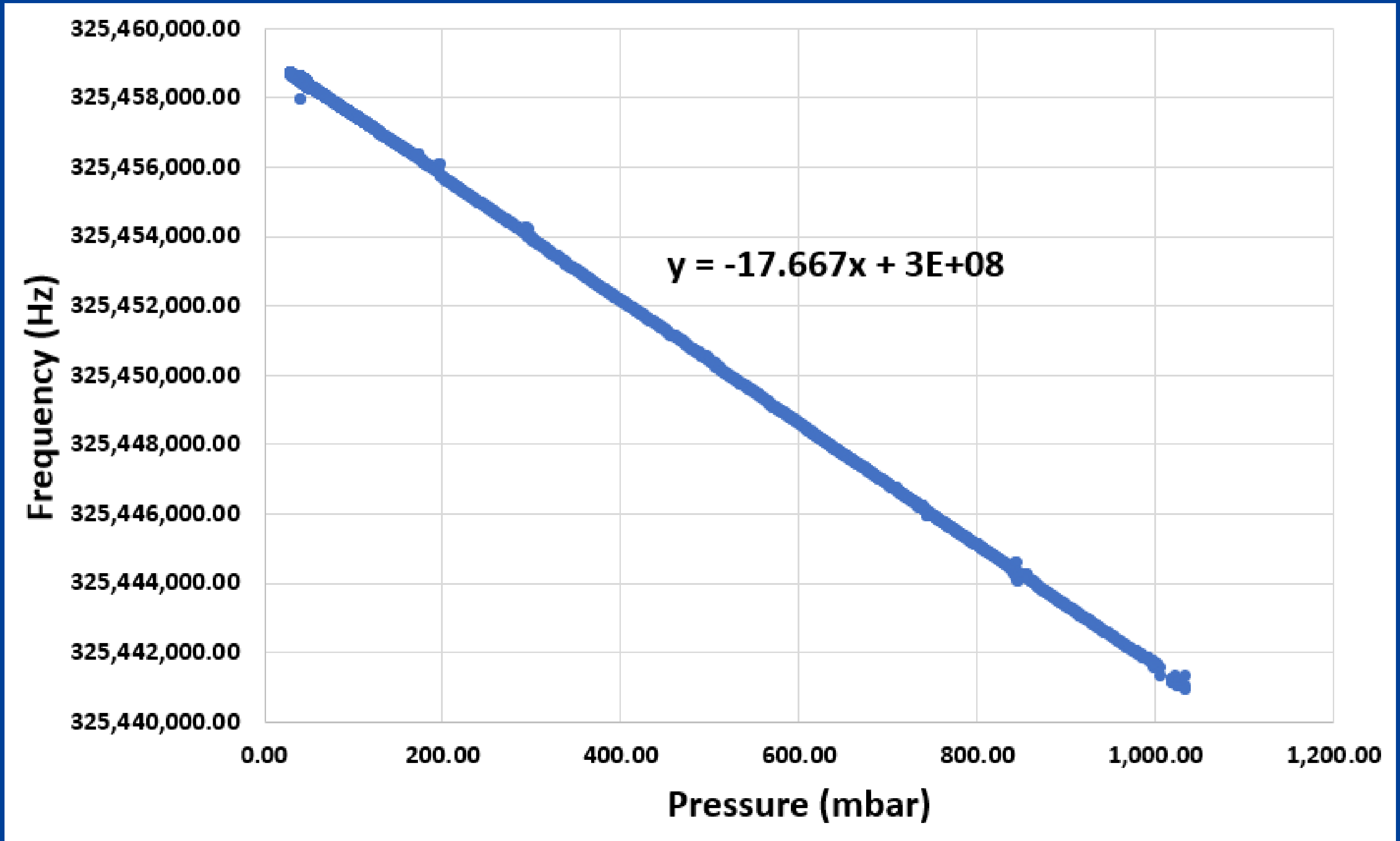

Figure: Resonance frequency as a function of pressure.

The measured pressure sensitivity is -17.67 Hz/mbar.

Compare Q Curves at 4.2 K with and without a RT Leak

iRiS 중이온가속기연구소 Institute for Rare Isotope Science

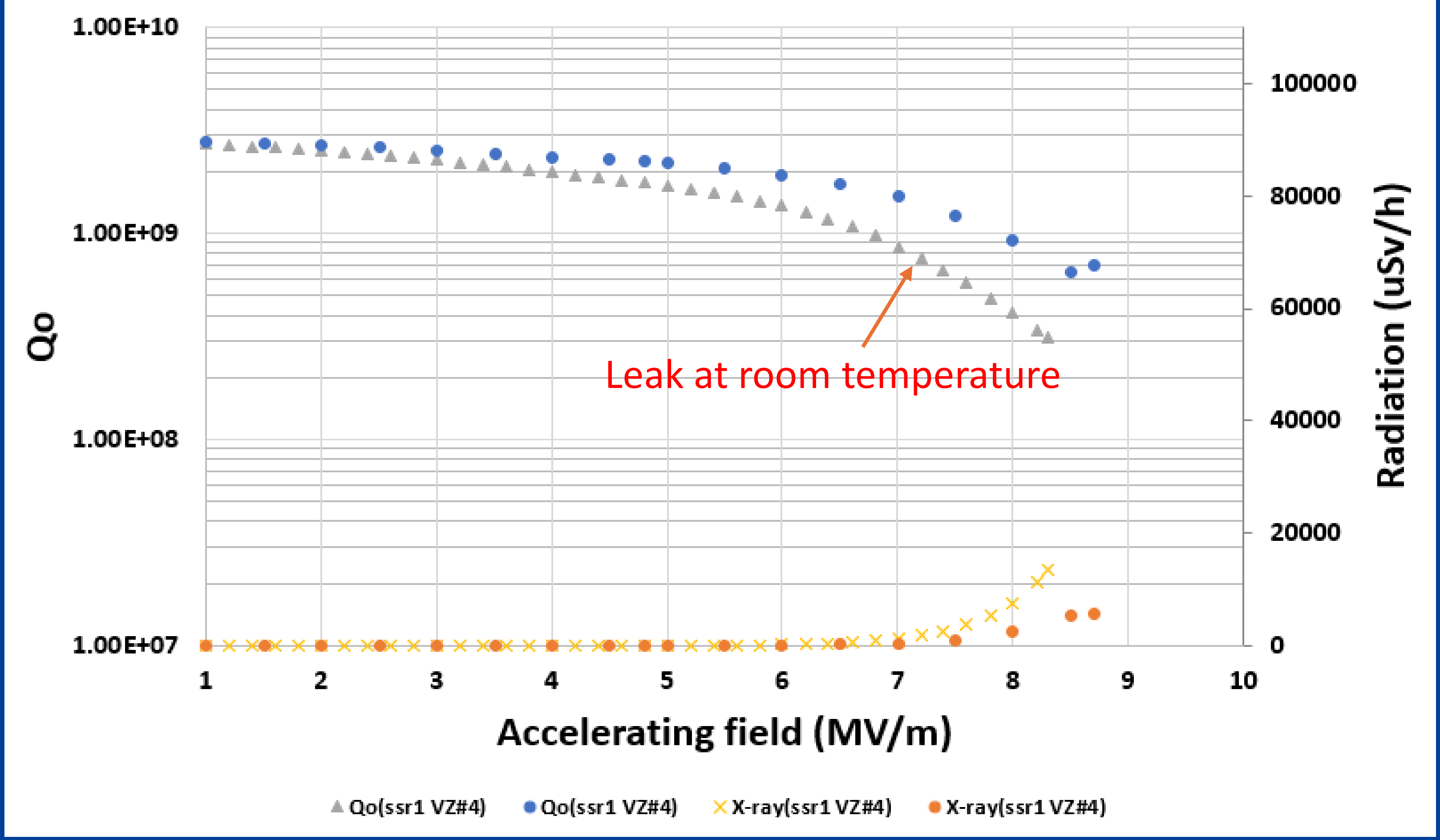

Figure: Q curves measured at 4.2 K with and without a room-temperature leak.
The presence of the leak leads to magnetic heating, caused by increased surface resistance due to residual gases.

Heetae Kim, Sungmin Jeon, Yoochul Jung, Juwan Kim, Magnetic heating effect for Quarter-Wave Resonator (QWR) superconducting cavities, *Quantum Beam Sci.* 7(3), 21 (2023).

Exit Velocity from a Nozzle

Nozzle diameter: $\mathrm{d} = 0.5\,\mathrm{mm} = 0.0005\,\mathrm{m}$

Pressure: $\mathrm{P} = 100\,\mathrm{bar} = 10^7$ Pa

Water density: $\rho = 1000\,\mathrm{kg/m^3}$

Assume ideal flow (incompressible, no friction loss) for initial estimation

Bernoulli’s Equation:

$$P_1 + \frac{1}{2}\rho v_1^2 + \rho g h_1 = P_2 + \frac{1}{2}\rho v_2^2 + \rho g h_2$$

$$P_1 = \frac{1}{2}\rho v_2^2 + P_2$$

$$\mathrm{P} = \frac{1}{2}\rho \mathrm{v}^2$$

$$\mathrm{v} = \sqrt{\frac{2\mathrm{P}}{\rho}}$$

Exit velocity is approximately $\mathrm{v} = 141.4$ m/s

Flow Rate and Force for the Water Jet

The volumetric flow rate (Q_{flow}) is given by:

$$Q_{flow} = A \times v$$

$$\mathrm{Q_{flow}} = (1.9635 \times 10^{-7}) \times 141.42 \approx 2.77 \times 10^{-5}\ \mathrm{m^3/s}$$

The volumetric flow rate (Q_{flow}) is $Q_{flow} = 2.77\ \mathrm{m\,L}/s$

The reaction force exerted by the water jet is the momentum change per unit time,

calculated using the mass flow rate and velocity:

$$F = \dot{m} \times v$$

$$\dot{m} = \rho \times Q_{flow}$$

The reaction force is $F = 0.02777 \times 141.42 \approx 3.93\ N$

Stokes' Drag Force for Low Reynolds Number

Stokes' drag for a water droplet in air:

$$F_d = 6\pi\eta r v$$

$$\eta(\text{viscosity of air}) \approx 1.81 \times 10^{-5}\ \text{Pa·s}\ \ (\text{at } 20°\text{C})$$

Stokes' drag for a superfluid helium droplet in helium vapor below 2.17 K:

$$F_d = 4\pi\eta r v$$

Stokes' drag is applicable to slow-moving, micron-sized particles and is valid in low Reynolds number (Re < 1) regimes.

H. Kim, K. Seo, B. Tabbert, G. A. Williams, Properties of Superfluid Fog, Europhys. Lett. 58(3), 395-400 (2002).

Quadratic Drag Force for Turbulent Flow

Reynolds number for the jet's diameter:

$$\mathrm{Re} = \frac{\rho v d}{\eta}$$

$$\mathrm{Re} = \frac{1.2 \times 141.42 \times 0.0005}{1.81 \times 10^{-5}} \approx 4700$$

High Re means turbulent flow, where quadratic drag is more appropriate.

For high-speed objects in turbulent flow, the drag force is:

$$F_d = \frac{1}{2} C_d \rho_{air} A v^2$$

- C_d(drag coefficient) ≈ 0.47 for a sphere, typical for droplets)
- ρ_{air} = 1.2 kg/m³ (air density)
- A = cross-sectional area of the droplet
- v = velocity at a given time

Velocity Calculation for Quadratic Drag

The net force on the droplet is the drag force opposing motion:

$$m\frac{dv}{dt} = -F_d$$

$$\frac{dv}{dt} = -0.846v^2 \qquad k = 0.846\ \mathrm{s/m}$$

$$\frac{dv}{v^2} = -k\,dt$$

Solve for velocity as a function of time:

$$\int_{v_0}^{v}\frac{dv'}{v'^2} = -k\int_0^t dt$$

$$v = \frac{v_0}{1 + v_0 kt}$$

$$v(t) = \frac{141.42}{1 + 119.64t}$$

Velocity Calculation at a Given Distance

Distance traveled :

$$x = \int_0^t v(t')\ dt'$$

$$x \approx 1.182\ln(1 + 119.64t)$$

Time :

$$t = \frac{e^{x/1.182} - 1}{119.64}$$

Velocity :

$$v = \frac{141.42}{1 + 119.64t}$$

Calculate velocity at 10 cm:

$$t = \frac{e^{0.1/1.182} - 1}{119.64} \approx 0.000737\ \mathrm{s}$$

$$v = \frac{141.42}{1 + 119.64 \times 0.000737} \approx 130.00\ \mathrm{m/s}$$

Velocity vs. Distance for a Water Droplet

Distance (cm)	Velocity (m/s)
10	130.00
20	119.41
30	109.71
40	100.85
50	92.64

Table: Velocity of a water droplet as a function of distance traveled.

The velocity decreases rapidly with increasing distance due to drag forces acting on the droplet.

Droplet Breakup and Jet Spreading Considerations

To enhance the realism of our high-pressure water jet model (initial velocity: 141.42 m/s, nozzle diameter: 0.5 mm), we incorporate additional physical effects:

Droplet Breakup:
As the jet travels, large droplets fragment into smaller ones. This increases the total surface area, which in turn increases drag and reduces velocity more rapidly.

Jet Spreading:
As the jet propagates, it expands radially due to internal turbulence and air resistance. This widens the spray angle, altering how the water interacts with the surface and surrounding air.

These effects become increasingly significant over distances of 10 cm, 20 cm, 30 cm, 40 cm, and 50 cm, and should be included in simulations for accurate modeling of high-pressure rinsing dynamics.

High Pressure Rinsing (HPR) Simulation Information

- Mesh Details for SSR1 Cavity:
  - Total mesh count: 249,252
  - Total surface area: 1.1132 m^2
  - Minimum mesh area: 0.92 mm^2
  - Maximum mesh area: 8.62 mm^2
  - Average mesh area: 4.47 mm^2

- Angular Scan Interval: 0.3°
- Nozzle Path Configuration:
  - 1 beam port axis
  - 2 coupler port axes
  - 4 tilted off-axis paths

- Nozzle Specifications:
  - Diameter: 0.5 mm
  - Cross-sectional area: 0.196 mm^2
  - Coverage ratio *(Avg. mesh area / nozzle area)*: 22.7

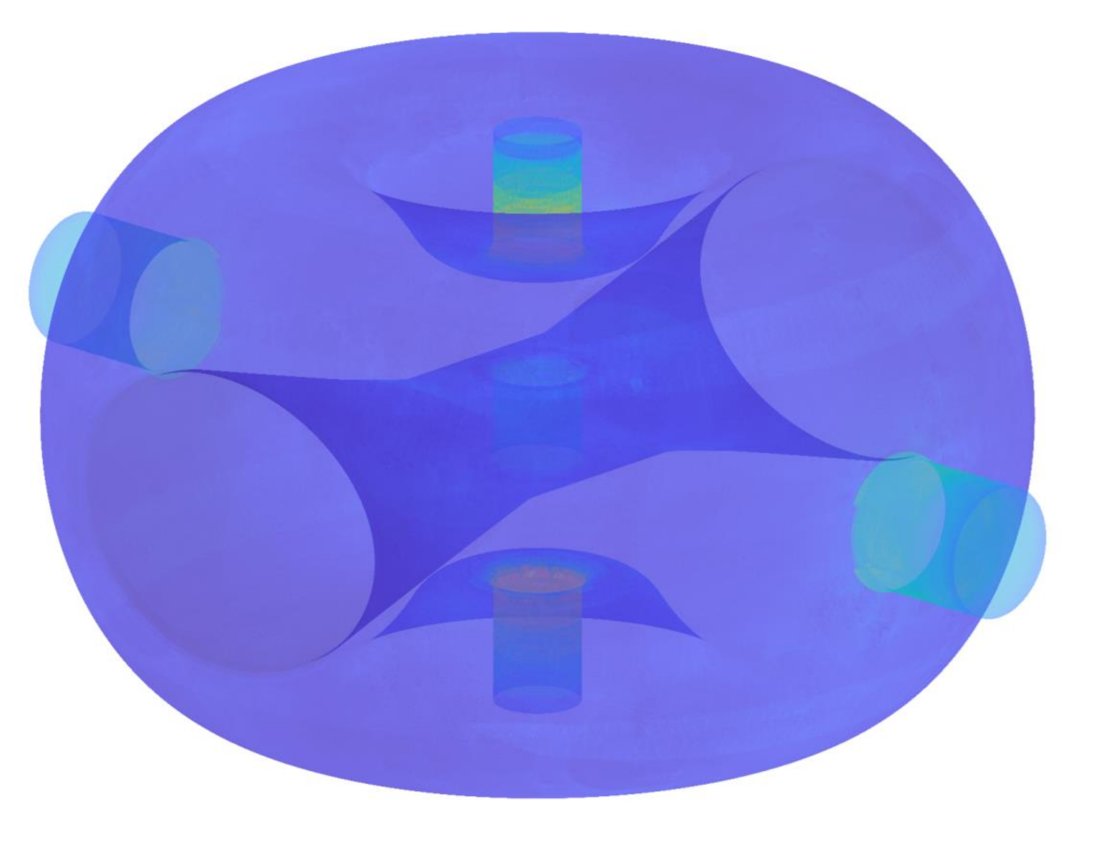

Figure: SSR1 superconducting cavity.

Simulation performed by Juwan Kim

High Pressure Rinsing Simulation

In order to improve HPR, we try to increase the water pressure by reducing the number of nozzles' hole.

Side port nozzle (22 holes)

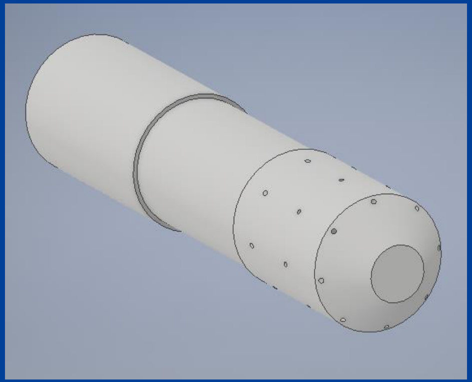

Beam port nozzle (24 hole)

Nozzle (16 holes)

HPR Rinsing Path

iRiS 중이온가속기연구소 Institute for Rare Isotope Science

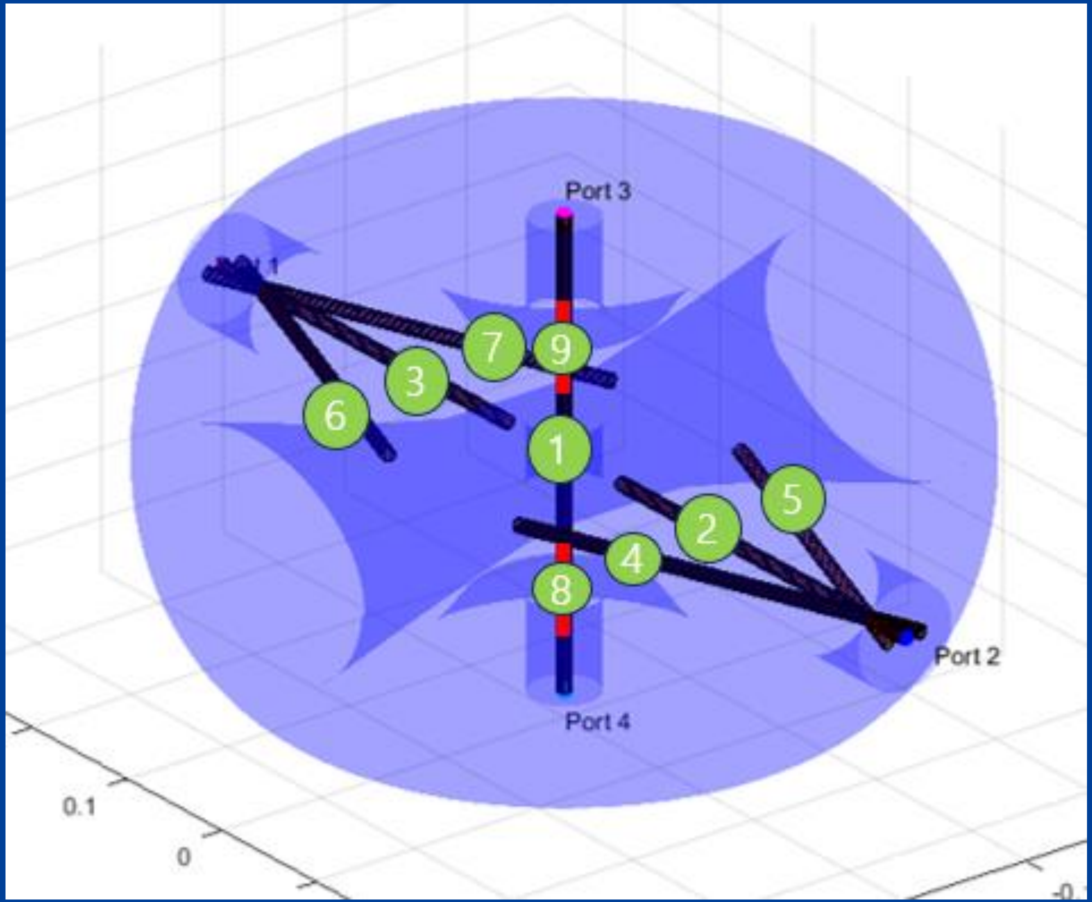

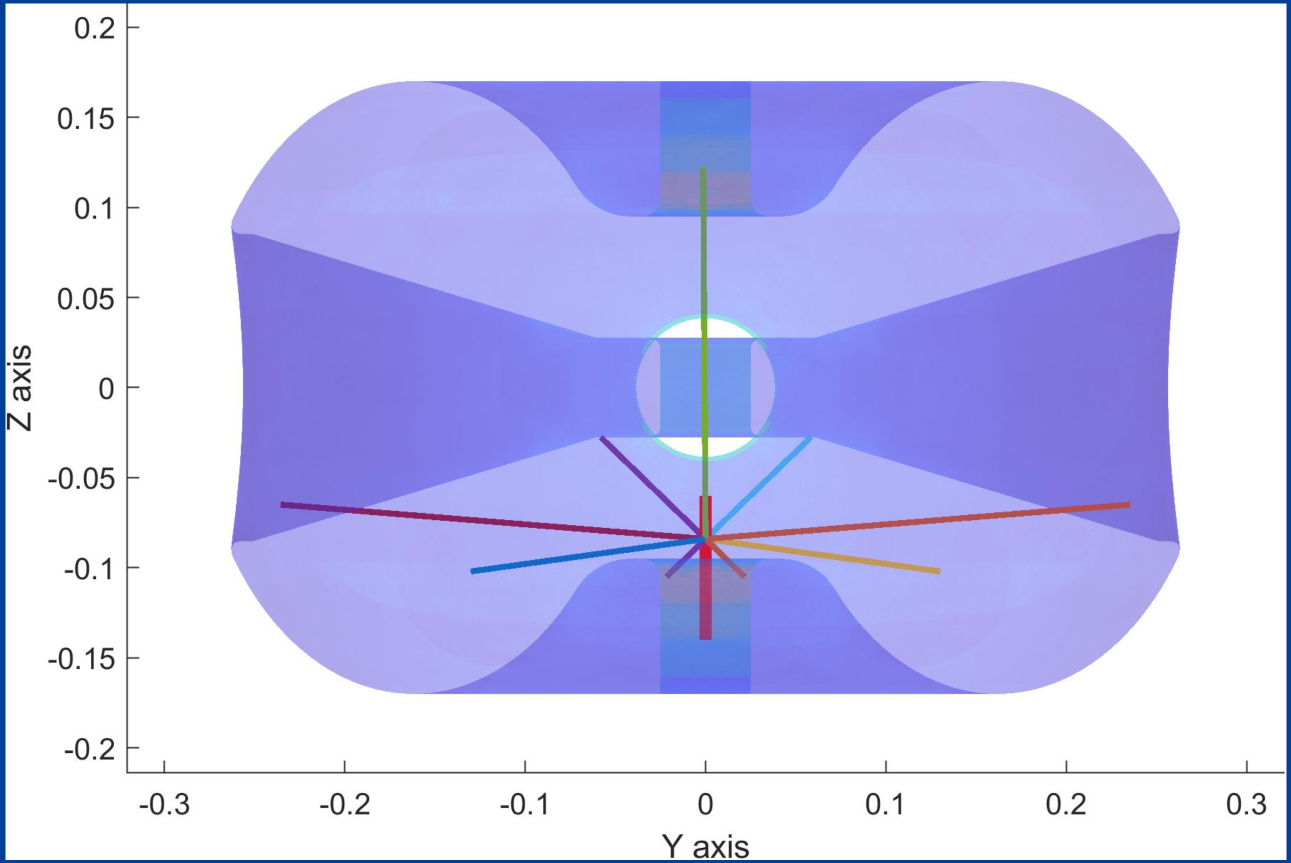

Figure: HPR rinsing paths.

Nozzle Models for HPR Simulations

Previous model (22 holes)

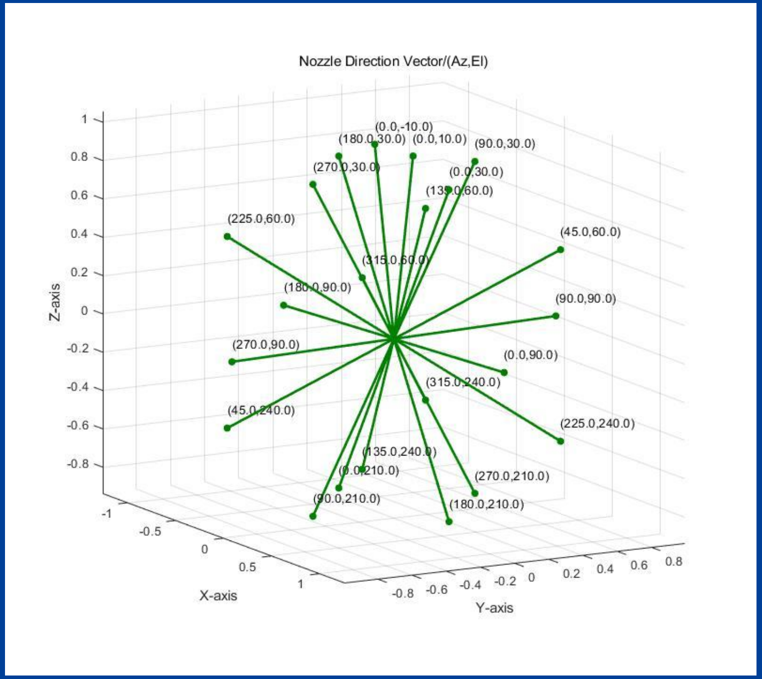

Previous model (24 holes)

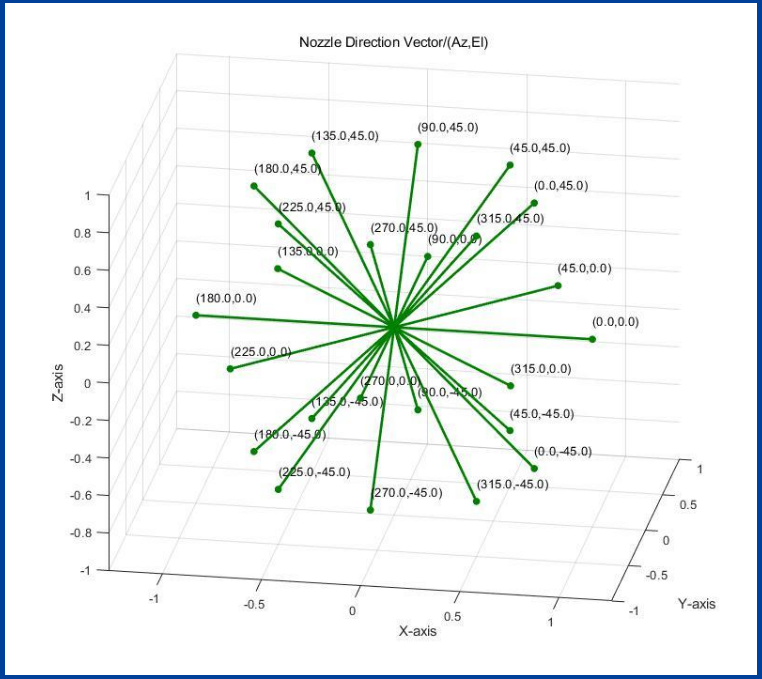

Updated model (16 holes)

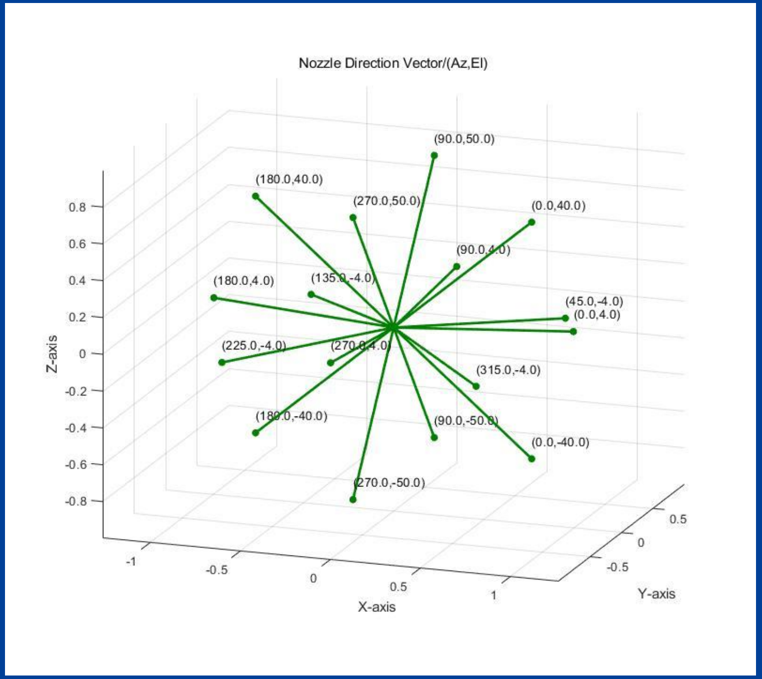

Figure: Directions of water jet from a nozzle.

The diagrams illustrate the spray angles and orientation of jets in both the previous and updated nozzle designs.

Simulation Results for HPR

iRiS 중이온가속기연구소 Institute for Rare Isotope Science

Content	Previous HPR Simulation	Updated HPR Simulation for 16 holes
Coverage	99.73	99.71
Path Information	Path List: 1, 10, 11, 2, 3, 4, 5, 6, 7, 1	Path List: 1, 2, 3, 4, 5, 6, 7, 8, 9, 1
Number of nozzle holes	24(beam port), 22(side port)	16 (beam port and side port)
Revolution/minute	10	10
Translation/minute	5 cm/min	5 cm/min

Simulation Results for HPR

iRIS 중이온가속기연구소 Institute for Rare Isotope Science

Previous model

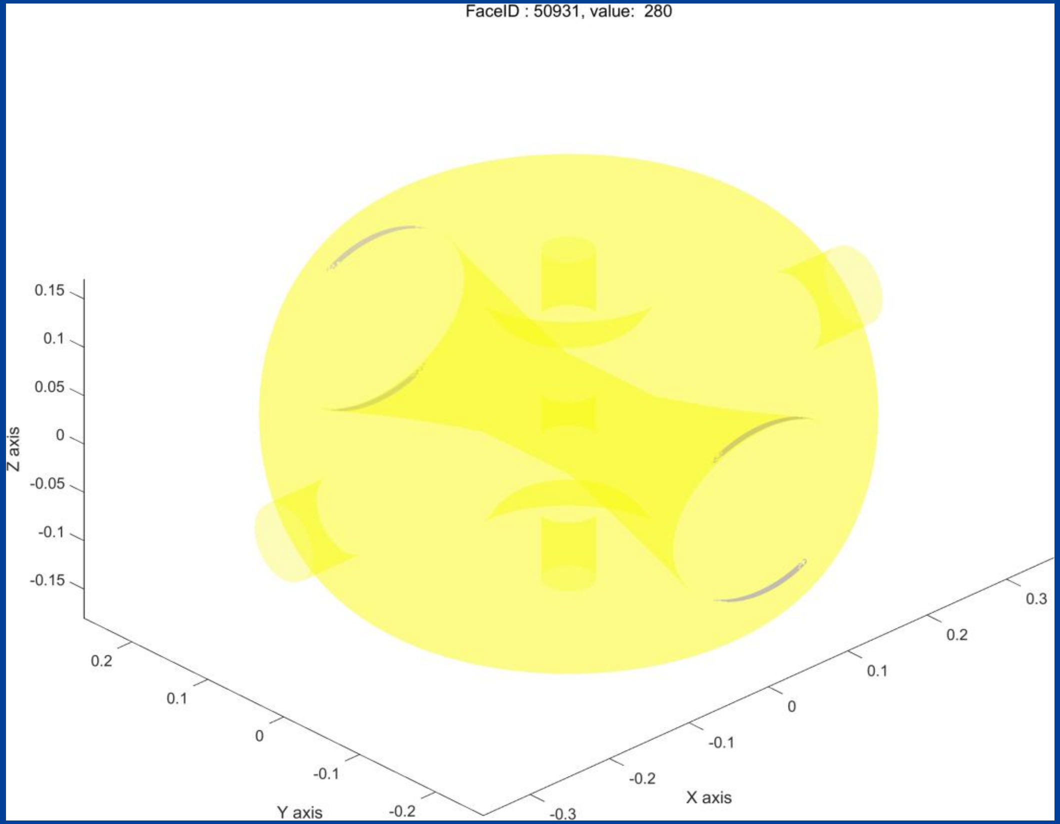

Updated model (16 holes)

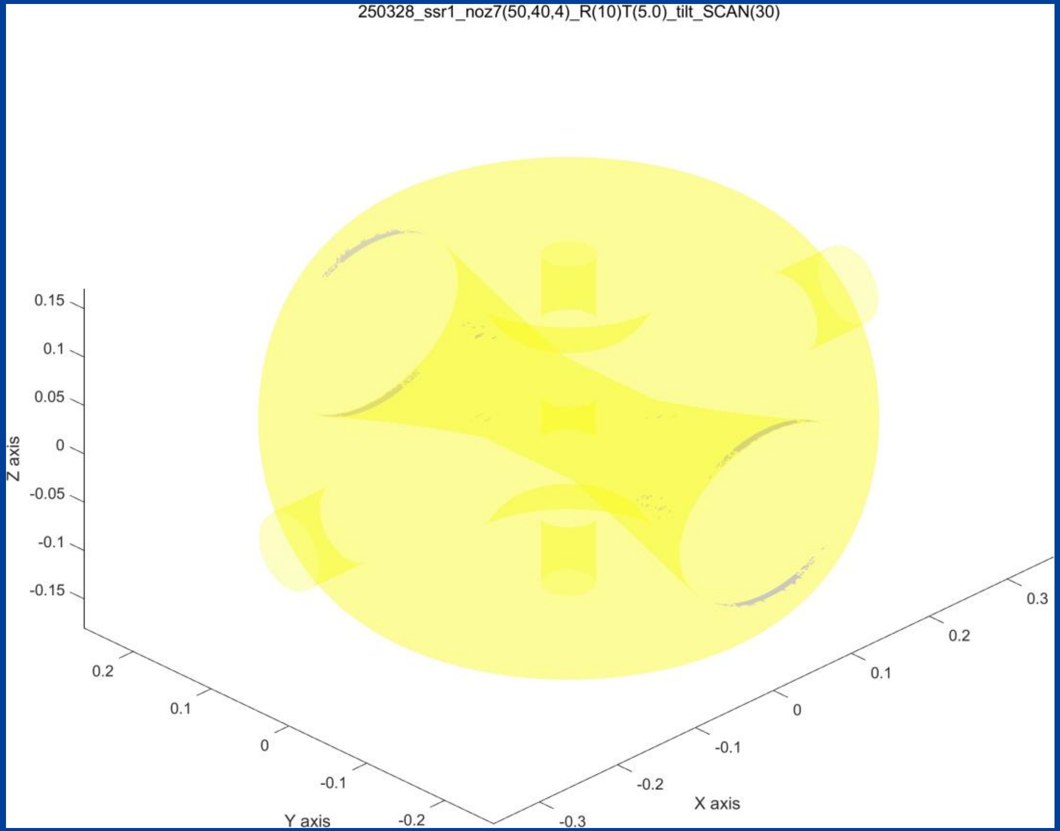

Figure: Untouched regions of the SSR1 cavity by the water jet during high-pressure rinsing.

Improvements are required in these areas to ensure full surface coverage and effective cleaning.

Summary

- The vertical test facility setup was presented.
- Performance test results for SSR1 cavities were discussed, with two cavities successfully passing qualification.
- The fundamental theory of water jet dynamics for high-pressure rinsing (HPR) was introduced, and droplet velocity was analyzed as a function of travel distance.
- HPR simulations were conducted to improve water jet impact on SSR1 cavity surfaces.
- Improvements are needed in regions that remain insufficiently covered to ensure full surface cleanliness and effective rinsing.

Thank you for your attention.

iRiS 중이온가속기연구소
Institute for Rare Isotope Science

대전광역시 유성구 국제과학로 1
1, Gukjegwahak-ro, Yuseong-gu, Daejeon, Korea